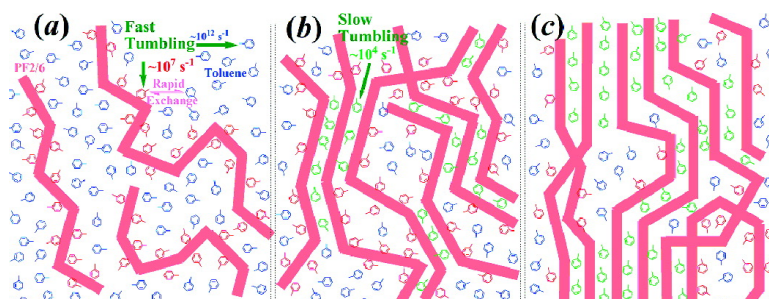


## Aggregation of Conjugated Polymers in Aromatic Solvent

M. Habibur Rahman, Shao-Ching Liao, Hsin-Lung Chen, Jean-Hong Chen, Viktor A. Ivanov, Peter P. J. Chu, and Show-An Chen

*Langmuir*, 2009, 25 (3), 1667-1674 • DOI: 10.1021/la802526d • Publication Date (Web): 02 January 2009

Downloaded from <http://pubs.acs.org> on February 19, 2009



### More About This Article

Additional resources and features associated with this article are available within the HTML version:

- Supporting Information
- Access to high resolution figures
- Links to articles and content related to this article
- Copyright permission to reproduce figures and/or text from this article

[View the Full Text HTML](#)



**ACS Publications**  
High quality. High impact.

Langmuir is published by the American Chemical Society, 1155 Sixteenth Street N.W., Washington, DC 20036

# Aggregation of Conjugated Polymers in Aromatic Solvent

M. Habibur Rahman,<sup>†,||</sup> Shao-Ching Liao,<sup>†</sup> Hsin-Lung Chen,<sup>†,\*</sup> Jean-Hong Chen,<sup>‡</sup>  
Viktor A. Ivanov,<sup>§</sup> Peter P. J. Chu,<sup>⊥,\*</sup> and Show-An Chen<sup>†</sup>

Department of Chemical Engineering, National Tsing Hua University, Hsinchu 30013, Taiwan;  
Department of Polymer Materials, Kun Shan University, Yungkuang City, Tainan Hsien 71003, Taiwan;  
Physics Department, Moscow State University, Moscow 117234, Russia; and Department of Chemistry,  
National Central University, Zhong-Li 32001, Taiwan

Received August 4, 2008. Revised Manuscript Received November 20, 2008

Segments of conjugated polymers display the propensity to aggregate in solutions with common organic solvents. Here we revealed that the segmental aggregation of a conjugated polymer, poly(9,9-bis(2-ethylhexyl)fluorene-2,7-diyl), (PF2/6), in toluene was stabilized by the polymer–solvent complex formation through  $\pi$ – $\pi$  stacking induction of solvent molecules and polymer segments. In this case, a portion of the solvent was trapped inside the aggregate domains upon bringing the system to the subambient temperatures. The residence time of these associated solvent molecules became long enough to yield a separate upfield-shifted NMR resonance. The line-shape of this resonance revealed alignment of the polymer segments in the aggregates. A portion of the solvent was frozen in the compact structure due to the formation of strong polymer–solvent complex.

## Introduction

$\pi$ -Conjugated polymers have been a critical component for the modern development of flexible electronics involving organic light-emitting diodes (OLEDs),<sup>1–5</sup> thin-film transistors (TFTs),<sup>6,7</sup> and photovoltaics.<sup>8–10</sup> Use of conjugated polymers in optoelectronic devices requires thin films to be cast from appropriate solutions. The solubility of the polymer is, however, restricted by the strong  $\pi$ – $\pi$  interaction and the large chain rigidity that greatly lowers the entropy of mixing. This problem is usually circumvented by attaching flexible short side chains to the conjugated backbone. Nevertheless, conjugated polymers are seldom molecularly dispersed in solution even through such a chemical modification. Abundant evidence have demonstrated that the conjugated segments tend to form submicrometer aggregate domains in the solutions.<sup>11–15</sup> The internal structure

of these aggregates and the nature of the interaction leading to the aggregation has however not been addressed unequivocally.

Here we resolve the type of interaction involved in the aggregation of conjugated polymers in aromatic solvent. A prototype of conjugated polymer, poly(9,9-bis(2-ethylhexyl)fluorene-2,7-diyl), (PF2/6), is adopted as the model system for the investigation. Polyfluorenes are a very attractive class of conjugated polymers due to their great potential uses in blue-light emitting devices.<sup>4,5,16</sup> In the bulk state polyfluorenes with sufficiently long side chains show a rich variety of self-organized structures, including nematic, hexagonal and lamellar phases, as well as a mesomorphic  $\beta$ -phase depending on the temperature, the backbone and side chain structures and the processing condition.<sup>17,18</sup> The self-organization is believed to be governed by the balance between the unfavorable backbone–side chain (rod–coil) interactions and the elastic stretching of the side chains; the former promotes microphase separation while the latter favors a homogeneous state.<sup>18</sup>

In the solution state, conformation of polyfluorene chains has been described as wormlike with the persistence length ( $l_p$ ) ranging between 7 and 10 nm.<sup>19–21</sup> They have been reported to dissolve down to the molecular level in dilute solutions of relatively good solvents (e.g., toluene and chloroform).<sup>15,19</sup> In semidilute solutions or more generally in poorer solvents, polyfluorenes undergo segmental aggregation. For instance, poly(9,9-dioctylfluorene-2,7-diyl) (PF8) in semidilute toluene solutions forms a dynamic

\* To whom correspondence should be addressed. E-mail: (H.-L.C.) hslchen@mx.nthu.edu.tw; (P.P.J.C.) ppjchu@gmail.com).

<sup>†</sup> National Tsing Hua University.

<sup>‡</sup> Kun Shan University.

<sup>§</sup> Moscow State University.

<sup>⊥</sup> National Central University.

<sup>||</sup> Present affiliation: Department of Chemistry, University of Rajshahi, Rajshahi 6205, Bangladesh (E-mail: psumhr@gmail.com).

(1) Friend, R. H.; Gymer, R. W.; Holmes, A. B.; Burroughes, J. H.; Marks, R. N.; Taliani, C.; Bradley, D. D. C.; Santos, D. A. D.; Brédas, J. L.; Lögdlund, M.; Salaneck, W. R. *Nature (London)* **1999**, *397*, 121–130.

(2) Grice, A. W.; Bradley, D. D. C.; Bernius, M. T.; Inbasekaran, M.; Wu, W. W.; Woo, E. P. *Appl. Phys. Lett.* **1998**, *73*, 629–631.

(3) Gross, M.; Müller, D. C.; Nothofer, H.-G.; Scherf, U.; Neher, D.; Bräuchle, C.; Meerholz, K. *Nature (London)* **2000**, *405*, 661–665.

(4) Neher, D. *Macromol. Rapid Commun.* **2001**, *22*, 1365–1385.

(5) Scherf, U.; List, E. J. W. *Adv. Mater.* **2002**, *14*, 477–487.

(6) Allard, S.; Forster, M.; Souharce, B.; Thiem, H.; Scherf, U. *Angew. Chem. Int. Edn.* **2008**, *47*, 2–31.

(7) Kline, R. J.; McGehee, M. D. *J. Macromol. Sci., Part C: Polym. Rev.* **2006**, *46*, 27–45.

(8) Hoppe, H.; Sariciftci, N. S. *J. Mater. Res.* **2004**, *19*, 1924–1945.

(9) Lv, X.; Mao, J.; Liu, Y.; Huang, Y.; Ma, Y.; Yu, A.; Yin, S.; Chen, Y. *Macromolecules* **2008**, *41*, 501–503.

(10) Zhan, X.; Tan, Z.; Domercq, B.; An, Z.; Zhang, X.; Barlow, S.; Li, Y.; Zhu, D.; Kippelen, B.; Marder, S. R. *J. Am. Chem. Soc.* **2007**, *129*, 7246–7247.

(11) Dias, F. B.; Morgado, J.; Macanita, A. L.; daCosta, F. P.; Burrows, H. D.; Monkman, A. P. *Macromolecules* **2006**, *39*, 5854–5864.

(12) Kitts, C. C.; Bout, D. A. V. *Polymer* **2007**, *48*(8), 2322–2330.

(13) Knaapila, M.; Almásy, L.; Garamus, V. M.; Ramos, M. L.; Justino, L. L. G.; Galbrecht, F.; Preis, E.; Scherf, U.; Burrows, H. D.; Monkman, A. P. *Polymer* **2008**, *49*, 2033–2038.

(14) Knaapila, M.; Dias, F. B.; Garamus, V. M.; Almásy, L.; Torkkeli, M.; Leppanen, K.; Galbrecht, F.; Preis, E.; Burrows, H. D.; Scherf, U.; Monkman, A. P. *Macromolecules* **2007**, *40*, 9398–9405.

(15) Knaapila, M.; Garamus, V. M.; Dias, F. B.; Almásy, L.; Galbrecht, F.; Charas, A.; Morgado, J.; Burrows, H. D.; Scherf, U.; Monkman, A. P. *Macromolecules* **2006**, *39*, 6505–6512.

(16) Leclerc, M. *J. Polym. Sci., Part A: Polym. Chem.* **2001**, *39*, 2867–2873.

(17) Peet, J.; Brocker, E.; Xu, Y.; Bazan, G. C. *Adv. Mater.* **2008**, *20*, 1882–1885.

(18) Stepanyan, R.; Subbotin, A.; Knaapila, M.; Ikkala, O.; Brinke, G. *Macromolecules* **2003**, *36*, 3758–3763.

(19) Fytas, G.; Nothofer, H. G.; Scherf, U.; Vlassopoulos, D.; Meier, G. *Macromolecules* **2002**, *35*, 481–488.

(20) Grell, M.; Bradley, D. D. C.; Long, X.; Chamberlain, T.; Inbasekaran, M.; Woo, E. P.; Soliman, M. *Acta Polym.* **1998**, *49*, 439–444.

(21) Knaapila, M.; Stepanyan, R.; Torkkeli, M.; Lyons, B. P.; Ikonen, T. P.; Almásy, L.; Foreman, J. P.; Serimaa, R.; Güntner, R.; Scherf, U.; Monkman, A. P. *Phys. Rev. E* **2005**, *71*, 041802. 4 Pt 1.

network structure having domains of aggregates of aligned segments<sup>22</sup> whereas in a poorer solvent methylcyclohexane (MCH), the polymer forms disk or sheet-like aggregates even in the dilute regime.<sup>14,15</sup>

The aggregation phenomena of conjugated polymers has always been a concern for their optoelectronic applications, as the presence of aggregates dramatically alters the photophysics of the material.<sup>23</sup> Considerable amount of study has been conducted in the past few years to understand the aggregate structure in relation to the photophysics of the polymers as a function of such variables as solvent quality, molecular weight, side-chain structure and length.<sup>12–15</sup> However, studies on the temperature dependence of the aggregation behavior<sup>11,22</sup> is scarce in the literature. These studies mainly utilized scattering techniques to discern the global aggregate structure and absorption and photoluminescence spectroscopy for identifying the effects of the aggregates on the photophysics. Nevertheless, the internal structure of these aggregates and the nature of interaction involved are still obscured because of the inherent limitations of the tools of investigation.

In this study we report a simple approach for resolving the mechanism of segmental aggregation of PF2/6 in toluene using <sup>1</sup>H NMR spectroscopy. This polymer tends to form aggregate domains at subambient temperatures. When the solution temperature is sufficiently low, a portion of the solvent gets encapsulated or bound within the aggregate domains of PF2/6. Isolation of the bound solvent from the bulk solution causes a separate upfield-shifted resonance line for the former. By analyzing the intensity and line-shape of this resonance, we are able to show that it is the  $\pi$ – $\pi$  stacking interaction between the solvent molecules and the polymer segments that stabilizes the aggregate domains. This greatly modifies the intuitive understanding that the aggregation of conjugated polymers in the solution state is driven by the  $\pi$ – $\pi$  interaction between the polymer segments.

## Experimental Section

Poly[9,9-bis(2-ethylhexyl)fluorene-2,7-diyl], (PF2/6) end-capped with dimethylphenyl groups was obtained from American Dye Source, Inc., Quebec, Canada. Its molecular weights were measured by GPC using THF as the eluting solvent against polystyrene standards. Most of the works in this study were carried out with the sample having  $M_w = 54600$  and PDI = 2.6. Another lower molecular weight polymer ( $M_w = 15000$  and PDI = 3.0) was also used for comparison purpose. Weighed amount of the PF2/6 was first dissolved in 0.5 mL toluene-*d*<sub>8</sub> (99.6 atom % <sup>2</sup>H, Cambridge Isotope Laboratories, Inc., U.S.A.) by gently warming in a water bath at 50 °C followed by stirring overnight at room temperature (*ca.* 25 °C). The solution was subsequently transferred into an NMR tube (5 mm diameter) and capped with silicon rubber septum. The concentration of the solution (g of polymer per 100 mL solution, %) was estimated from the height of the solution in the NMR tube calibrated to the volume. <sup>1</sup>H NMR measurements were conducted at 499.84 MHz on a Varian UnityInova-500 NMR spectrometer. For the observation of the development of aggregates at subambient temperatures, the sample was rapidly cooled to –20 or –30 °C and allowed to attain thermal equilibrium before acquiring the spectra (the process took 15 min at –20 °C and about 30 min at –30 °C inside the NMR instrument). <sup>1</sup>H NMR relaxation times of degassed (by bubbling dry N<sub>2</sub>) samples were measured by the inversion recovery pulse sequence, i.e.,  $\pi$ – $\tau_d$ – $\pi/2$ –acquire sequence, with  $\pi = 25.2 \mu\text{s}$ ,  $\tau_d$  ranging between 0.01 s and 64 s and a dead time of 40 s using the same instrument.

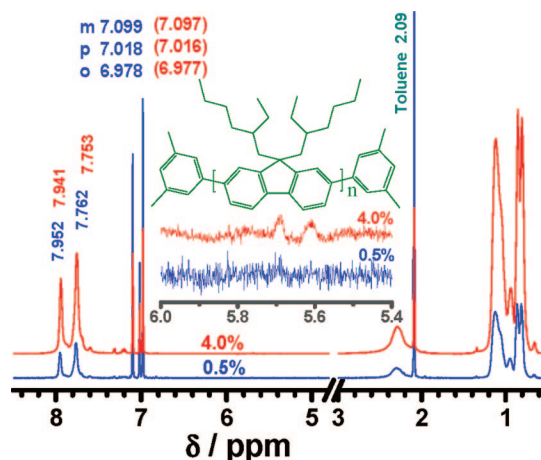


**Figure 1.** Representative 500 MHz <sup>1</sup>H NMR spectra of freshly prepared poly(9,9-bis(2-ethylhexyl)fluorene-2,7-diyl) (PF2/6) solutions in toluene-*d*<sub>8</sub> of indicated concentrations at 25 °C. A magnified view of the 5.4–6.0 ppm region and the chemical structure of the polymer used are also shown with the spectra.

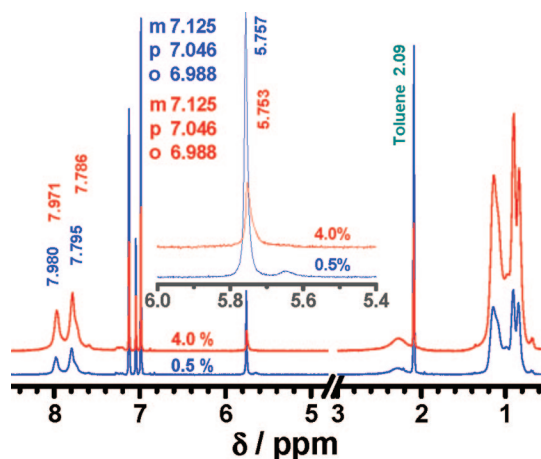


**Figure 2.** Representative 500 MHz <sup>1</sup>H NMR spectra of PF2/6 solutions in toluene-*d*<sub>8</sub> of indicated concentrations taken at –20 °C after cooling the solution from 25 °C in one step followed by thermal equilibration (which took about 15 min inside the NMR probe). The solvent lines are more intense for the 0.5% solution than those for the 4.0% solution, as expected, so is the intensity of the extra resonance lines (as the opposite is true for the PF2/6 line intensity). Inset: Magnified view of the extra resonance region.

## Results and Discussion

Figure 1 shows the 500 MHz <sup>1</sup>H NMR spectra of 0.5% and 4.0% solutions of PF2/6 in toluene-*d*<sub>8</sub> at 25 °C. Both spectra contain broad and overlapped resonance bands for the PF2/6 backbone aromatic and side-chain aliphatic protons and few sharp lines for the residual protons from toluene-*d*<sub>8</sub>. A small upfield shift in the polymer resonance bands can be identified for the 4.0% solution relative to the 0.5% one. Few small peaks can also be identified between 5.6 and 5.8 ppm in the spectrum of the 4.0% solution, which are below the detection limit in the spectrum of the 0.5% solution, as shown in the magnified window of the spectra in Figure 1.

Upon cooling to –20 °C from the ambient temperature, solutions with concentrations ranging between 0.5% and 5.3% all displayed an additional sharp resonance line at 5.75 ppm in <sup>1</sup>H spectra. Spectra of 0.5% and 4.0% solutions are shown in Figure 2 as representative. It is noted that the sharp line is absent in the room-temperature spectra, although a few weak resonances can be observed in the same region of the spectrum of the 4.0%

(22) Rahman, M. H.; Chen, C. Y.; Liao, S. C.; Chen, H. L.; Tsao, C. S.; Chen, J. H.; Liao, J. L.; Ivanov, V. A.; Chen, S. A. *Macromolecules* **2007**, *40*, 6572–6578.

(23) Schwartz, B. J. *Annu. Rev. Phys. Chem.* **2003**, *54*, 141–172.



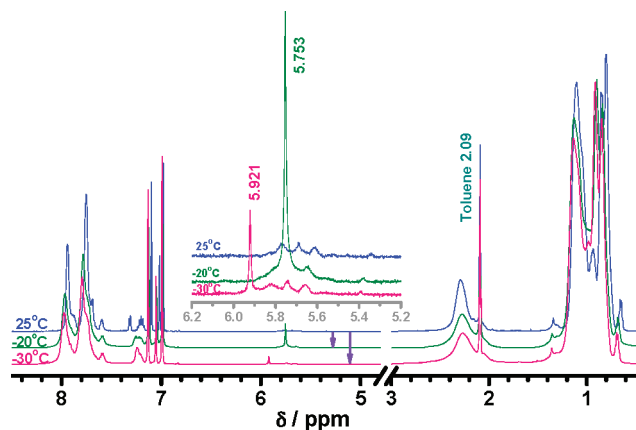


**Figure 3.** 500 MHz  $^1\text{H}$  NMR spectra of a 5.0% solution of PF2/6 ( $M_w = 15000$ , PDI = 3) in toluene- $d_8$  taken after cooling from room temperature to either  $-30$  or  $-20$   $^\circ\text{C}$  in one step.

solution (Figure 1). From the relative intensity and the sharpness, this extra resonance is attributed to residual aromatic proton of the solvent.<sup>22</sup>

Appearance of the extra resonance from solvent proton indicates the formation of an additional magnetic environment for the solvent at subambient temperatures. This can be attributed to entrapment of a fraction of the solvent molecules within the aggregate domains of PF2/6, where aggregate formation is supported by at least 10% to 24% decrease of the normalized relative intensity of the polymer resonances (see below) arising from the loss of motional narrowing due to steric constraints of the polymer backbone motions caused by the aggregation.<sup>24</sup> It will be shown later (in Figure 5) that the resonance at 5.75 ppm gradually decays with time, confirming its association with the solvent trapped (bound) within the aggregate domains that diffuses out on aging. Contrary to the common understanding of a polymer solution where the solvent molecules are under rapid exchange between the solvated polymer and the bulk solvent, here we find that a fraction of the solvent is actually bound or associated with the polymer segments in the aggregate domains. The residence time of the associated solvent (roughly inversely proportional to the exchange rate) becomes long enough to yield an NMR resonance separated from that of the bulk solvent. A most plausible force of the association originates from the induction of ring current between the aromatic ring of the solvent and that of the fluorene unit (i.e., the so-called  $\pi$ - $\pi$  stacking interaction).<sup>25,26</sup> Such stacking induction is very common in aromatic compounds and manifested in the upfield chemical shift for nuclei located at positions normal to the ring plane.<sup>27-29</sup> In the present case the polymer-solvent  $\pi$ - $\pi$  stacking interaction is prominent in the aggregate domains and as such, the residual aromatic protons of the solvent bound inside the aggregate domains suffer an upfield shift of about 1.3 ppm from those of the free solvent outside the aggregates. The fate of the aromatic resonances of the polymer segments in the aggregate phase is not immediately evident as they behave like solid spins (loss of

motional narrowing), consequently they do not show up in the spectra. However, the polymer segments in the bulk solution phase also interact through the  $\pi$ - $\pi$  stacking induction, albeit weakly. The extent of this interaction is increased at higher concentrations, which is clearly reflected in the upfield shift of about 0.01 ppm of the aromatic resonances of PF2/6 (between 7.7 and 8.0 ppm) as a result of the 8-fold increase in the solution concentration (Figures 1 and 2).

We would like to mention here that polymer-polymer  $\pi$ - $\pi$  stacking interaction is unfavorable in larger dialkyl substituted polyfluorenes<sup>30</sup> because the steric interactions posed by the alkyl side-groups hinder the backbone segments from being close enough for the  $\pi$ - $\pi$  stacking to be effective; a branching in the side-chain is likely to enhance this effect further. However, in conjugated polymer systems where the steric interaction is small or absent, polymer-polymer  $\pi$ - $\pi$  stacking is the main driving force for organization in the condensed phases.<sup>31</sup> We also mention here an interesting system where fluorene moieties pendent from an oligo-ethylene backbone through the C9 position of fluorene stack in cofacial juxtaposition geometry through  $\pi$ - $\pi$  interaction.<sup>28</sup> Here the proton resonances of the sandwiched central fluorene moiety suffer more upfield shift than the two outer fluorene moieties due to coupling of the  $\pi$  system. Similar coupling might have occurred in the aggregate domains due to the localization of the toluene molecules sandwiched between two parallel polymer segments acting as a bridge between them facilitating the alternate stacking of the monomer units and the solvent molecules via effective polymer-solvent-polymer  $\pi$ - $\pi$  interaction. We have observed a similar situation in poly(9,9-dioctylfluorene-2,7-diyl) (PF8) system<sup>22</sup> where the polymer in toluene solutions at concentrations exceeding 1% formed aggregate domains through a  $\pi$ - $\pi$  interaction that can sustain temperatures as high as 75  $^\circ\text{C}$ , whereas no aggregation was observed in tetrahydrofuran solutions even at ambient temperatures, although the  $\pi$ - $\pi$  interaction between the aromatic moieties of the polymer should be more favorable in the aliphatic solvent due to solvophobic interaction. Consequently, the present study and the mentioned previous work reveal that the polymer-solvent  $\pi$ - $\pi$  interaction is the dominant force that stabilizes the aggregates of conjugated polymers in aromatic solvents. This is a unique situation in the sense that it contradicts the chemist's familiar *like dissolves like* phenomenon by which an aromatic solvent is likely to solvate the aromatic conjugated backbones of the polymer rather than stabilizing their aggregation.

Most conjugated polymers aggregate obviously in the solution state when the solvent quality is lowered by adding a poor solvent or reducing the temperature. The aggregation phenomenon has been identified most noticeably in absorption and photoluminescence emission spectra manifested by a red-shift in the absorption and emission bands and a large drop in the quantum yield of the photoluminescence.<sup>32</sup> The loss of the quantum yield is due to the predominant interchain excitations of negligible luminescence due to close proximity of the segments when the polymer aggregates. The red shift is a consequence of increased conjugation length of the polymer backbone upon aggregation. Such an increase in the conjugation length implies that the rodlike segments should arrange relatively parallel to each other in the aggregate domains analogous to the liquid crystalline (LC) phases formed by rodlike molecules. In fact the aggregates of PF8 formed

(24) Collison, C. J.; Rothberg, L. J.; Treemanekarn, V.; Li, Y. *Macromolecules* **2001**, *34*, 2346-2352.

(25) Hunter, C. A.; Lawson, K. R.; Perkins, J.; Urch, C. J. *J. Chem. Soc., Perkin Trans.* **2001**, 651-669.

(26) Hunter, C. A.; Sanders, J. K. M. *J. Am. Chem. Soc.* **1990**, *112*, 5525-5534.

(27) Niazimbetova, Z. I.; Christian, H. Y.; Bhandari, Y. J.; Beyer, F. L.; Galvin, M. E. *J. Phys. Chem. B* **2004**, *108*, 8673-8681.

(28) Rathore, R.; Abdelwahed, S. H.; Guzei, I. A. *J. Am. Chem. Soc.* **2003**, *125*, 8712-8713.

(29) Shetty, A. S.; Zhang, J.; Moore, J. S. *J. Am. Chem. Soc.* **1996**, *118*, 1019-1027.

(30) McFarlane, S.; McDonald, R.; Veinot, J. G. C. *Acta Crystallogr. C* **2005**, *C61*, o671-o673.

(31) Li, Y. C.; Chen, K. B.; Chen, H. L.; Hsu, C. S.; Tsao, C. S.; Chen, J. H.; Chen, S. A. *Langmuir* **2006**, *22*, 11009-11015.

(32) Menon, A.; Galvin, M.; Walz, K. A.; Rothberg, L. *Synth. Met.* **2004**, *141*, 197-202.

in dilute methylcyclohexane solutions at below ambient temperatures have been described as anisotropic ordered domains of lamellar phases, somewhat similar to the lamellar structures of ordered smectic phases, rather than true crystallites.<sup>11</sup> Under the influence of the magnetic field of the NMR spectrometer, these segments should tend to orient their long axis along the magnetic field direction in a manner similar to the liquid crystal phases or the lipid based bicelles in aqueous dispersion.<sup>33–37</sup>

For individual solvent molecules or polymer segments, the energy required to tumble in the magnetic field for NMR measurements is small compared to the thermal energy; as a result, these molecules or segments would not orient in the magnetic field. However, an array of a large number of coupled or correlated molecules (such as in liquid crystals) or aligned segments of macromolecules (such as in the aggregates) should result in a magnetic torque large enough to induce appreciable orientational order in relatively low magnetic field strengths. The entrapped solvent molecules inside the aggregate domains would also gain a fixed orientation relative to the magnetic field. This is analogous to the study of the nuclear spin interactions of small molecules using liquid crystal solvent, where the system of interest is oriented in the liquid crystalline (director) phase that has been aligned with a fixed orientation relative to the magnetic field. Depending on the orientation of the individual interaction tensors (chemical shift, or dipolar coupling) and the relative orientation of the molecules with the external field, several sharp NMR absorptions occur over a wide range of frequencies.<sup>35,37–39</sup> This resonance hardly coincides with the motional averaged line of the molecule.

On the basis of the above discussion, it is apparent that the sharp line at 5.75 ppm for residual protons of associated toluene in Figure 2 is a consequence of the liquid crystal-like alignment of the polymer segments in the aggregate domains. The molecular ( $C_2$ ) axis of entrapped toluene gets a definite orientation relative to the magnetic field and the residual *para*-proton containing the said axis gives rise to the sharp resonance. The orientation of the  $C_2$  axis probably causes the resonances of the *ortho*- and the *meta*-protons to shift outside the measured frequency range, as a consequence they are not observed in the spectra. Such orientation, however, should cause numerous sharp, nonmotional-averaged resonance lines for *para*-proton of the associated toluene due to dipolar coupling with the neighboring protons. Observing only one of them located between 5 and 6 ppm means that no such dipolar interaction is effective. This is reasonable for the 99.6 atom % deuterated toluene used as the solvent. However, existence of such dipolar coupling could not be observed even when 2% (v/v) pure toluene was mixed with the deuterated solvent (see Figure 6 below). The plausible reason is that the associated toluene molecules are transient (see below) and they exchange with the nonassociated ones at a rate which is fast compared to the proton dipolar coupling constants, resulting in decoupling.<sup>40</sup> The exchange rate, however, is slow enough on the chemical

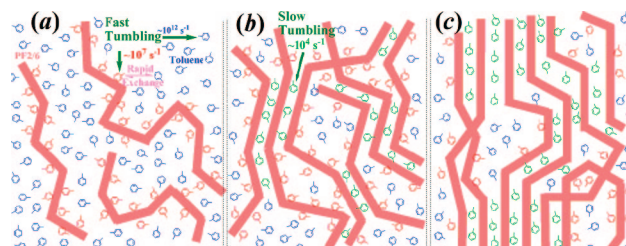


**Figure 4.** Proposed solution structure of PF2/6 in toluene.

shift time scale to display separate resonances, as mentioned earlier.

If the toluene molecules were associated within aggregates consisting of randomly oriented segments, they would not take a definite orientation with respect to the magnetic field direction; in which case the motional averaged three-line shape of the residual aromatic proton resonance of deuterated toluene should be identified. This is indeed observed in the room-temperature spectrum of the 4.0% solution (inset of Figure 1) in the same region where a small extent of such aggregates is present in the solution.

The association of the solvent within the aggregates of randomly oriented segments formed at room temperature is more clearly evident in case of a 5.0% solution of a PF2/6 sample of lower molecular weight ( $M_w = 15000$ , PDI = 3), as shown in Figure 3. When the temperature is lowered to  $-20\text{ }^\circ\text{C}$ , the sharp line for the oriented toluene associated with the newly formed aggregates appears at 5.75 ppm that superposes on the three solvent lines existing in the room-temperature spectrum. If the temperature is lowered to  $-30\text{ }^\circ\text{C}$  instead, the extra resonance line appears at a downfield shifted position whereas the position of the three-lines of the solvent associated with room-temperature aggregates suffer only little perturbation, allowing clear visualization of the coexistence of two contrasting types of aggregates, i.e., the one formed during solution preparation at room temperature has randomly oriented segments and the other developed during the cooling in the NMR probe has most of the segments aligned their long axis parallel to each other. This is an important finding in that the magnetic field actually induces alignment of the segments in the aggregate domains. This finding also has the far reaching practical consequence as a convenient method for producing oriented films of conjugate polymers from solutions under the influence of a magnetic field,<sup>41</sup> which are of interest for applications in field-effect transistors (FETs)<sup>42,43</sup> and the light-emitting diodes (LEDs) for linearly polarized electroluminescence.<sup>44,45</sup>

The 0.17 ppm less upfield shift for the associated solvent line at  $-30\text{ }^\circ\text{C}$  relative to that at  $-20\text{ }^\circ\text{C}$  is likely due to the change of the orientation of the  $C_2$  axis toward the magic angle ( $54.7^\circ$ ) as a consequence of the temperature drop, and hence leads to the shift of the line toward the isotropic value. There is also a compaction of the segments due to the temperature drop that limits the space for accommodating the solvent molecules in the aggregates, causing a reduction in the intensity of the associated solvent line at  $-30\text{ }^\circ\text{C}$  relative to that at  $-20\text{ }^\circ\text{C}$ .

(33) Alba, E. d.; Tjandra, N. *Prog. Nucl. Magn. Reson. Spectrosc.* **2002**, *40*, 175–197.

(34) Bax, A. *Protein Sci.* **2003**, *12*, 1–16.

(35) Brunell, E. E.; de Lange, C. A. *NMR of Ordered Liquids*; Springer: Berlin, 2003.

(36) Lipsitz, R. S.; Tjandra, N. *Annu. Rev. Biophys. Biomol. Struct.* **2004**, *33*, 387–413.

(37) Vivekanandan, S.; Joy, A.; Suryaprakash, N. *J. Mol. Struct.* **2004**, *694*, 241–247.

(38) Diehl P.; Khetrapal, C. L. *NMR Studies of Molecules Oriented in the Nematic Phase of Liquid Crystals*. In *NMR Basic Principles and Progress*; Diehl, P., Fluck, E., Kosfeld, R., Eds.; Springer-Verlag: Berlin, 1969; Vol. 1, pp 1–95.

(39) Meiboom, S.; Snyder, L. C. *Science* **1968**, *162*(3860), 1337–1345.

(40) Sanders, J. K. M.; Hunter, B. K. *Modern NMR Spectroscopy, A Guide for Chemists*; 2nd ed.; Oxford University Press: Oxford, U.K., 1993.

(41) Christianen, P. C. M.; Shklyarevskiy, I. O.; Boamfa, M. I.; Maan, J. C. *Physica B* **2004**, *346–347*, 255–261.

(42) Siringhaus, H.; Wilson, R. J.; Friend, R. H.; Inbasekaran, M.; Wu, W.; Woo, E. P.; Grell, M.; Bradley, D. D. C. *Appl. Phys. Lett.* **2000**, *77*, 406–408.

(43) Yasuda, T.; Fujita, K.; Tsutsui, T.; Geng, Y.; Culligan, S. W.; Chen, S. H. *Chem. Mater.* **2005**, *17*, 264–268.

(44) Grell, M.; Knoll, W.; Lupo, D.; Meisel, A.; Miteva, T.; Neher, D.; Nothofer, H.-G.; Scherf, U.; Yasuda, A. *Adv. Mater.* **1999**, *11*(5), 671–675.

(45) Nothofer, H.-G.; Meisel, A.; Miteva, T.; Neher, D.; Forster, M.; Oda, M.; Lieser, G.; Sainova, D.; Yasuda, A.; Lupo, D.; Knoll, W.; Scherf, U. *Macromol. Symp.* **2000**, *154*, 139–148.

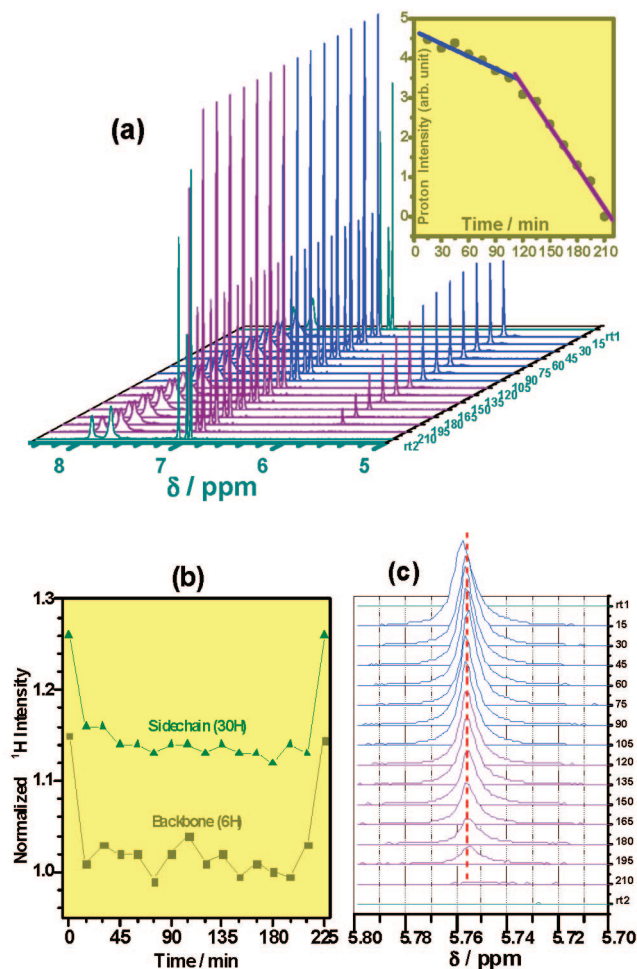


**Figure 5.** (a) 500 MHz  $^1\text{H}$  NMR spectra of 0.50% PF2/6 solution in toluene- $d_8$  taken for the fresh solution at 25  $^\circ\text{C}$  (rt1), at 15-min intervals during aging (corresponding time in minutes shown along the  $z$ -axis) at  $-20$   $^\circ\text{C}$  and after heating back to 25  $^\circ\text{C}$  (rt2). Inset: The intensity of the associated solvent line at 5.75 ppm as a function of time relative to the intensity of the solvent residual  $\text{CH}_3$  proton signal of the first spectra taken after cooling to  $-20$   $^\circ\text{C}$ . The solid lines are linear fits of the data (ranges differentiated by colors). (b) Integrated  $^1\text{H}$  intensities of PF2/6 backbone and side chain (centered at  $\sim 1$  ppm) lines normalized to the intensity of the residual  $-\text{CH}_3$  proton signal of toluene- $d_8$  at 2.09 ppm as a function of the annealing time at  $-20$   $^\circ\text{C}$ . The terminal data points at 0 and 225 min correspond to the room temperature spectra of the fresh solution and after reheating, (i.e., rt1 and rt2) respectively. Intensity values higher than unity may be due to contributions from the end groups (see structure in Figure 1) and from any uncertainty in the concentration. (c) Magnified view of the bound solvent line showing a small upfield shift and larger width at half-maximum with increasing annealing time.

The spectrum of the more dilute (0.5%) solution does not show aggregation to any detectable extent at 25  $^\circ\text{C}$  (inset of Figure 1). However, we see the trace of a broad second extra line next to the associated solvent line at  $-20$   $^\circ\text{C}$  (inset of Figure 2). This is probably because in this more dilute solution, the polymer segments in the aggregate domains are relatively less crowded providing even more space for the associated solvent molecules where some of them may tumble to some extent thus partially averaging the shift anisotropy for the protons in them, and consequently results in the small second extra resonance.

Apart from the chemical shift difference, the entrapped solvent molecules also display difference in spin–lattice relaxation time ( $T_1$ ). The  $^1\text{H}$  spin–lattice relaxation times of the residual protons in deuterated toluene for the 4.0% PF2/6 solution measured under the same experimental conditions at  $-20$   $^\circ\text{C}$  are given in Table

1. The  $T_1$  value for the entrapped solvent resonance is an order of magnitude shorter than the other solvent proton resonances, which is indicative of a much slower rotational dynamics of the solvent molecules. This is consistent with the notion of an association of these solvent molecules with the polymer segments through  $\pi$ – $\pi$  stacking in the aggregates.

It turns out that solutions of PF2/6 with toluene at subambient temperatures are complex fluids consisting of different types of aggregates and solvent dynamics. These are summarized in Table 2 and illustrated schematically in Figure 4. At room temperature, there is a low degree of aggregation in the dilute (0.5%) solution. The polymer chains (bold zigzag lines) are dispersed in the toluene matrix (Figure 4a). The predominant interaction here is the solvent–solvent  $\pi$ – $\pi$  and the polymer–solvent  $\pi$ – $\pi$  interaction. Due to the latter type of interaction, some solvent molecules (shown in red) probably spend more time near the segments and their dynamics is slowed down to some extent, but they exchange with the free molecules rapidly enough on the NMR time scale to show the motional narrowed residual proton resonances in NMR. In the more concentrated solution (4.0%), the scenario is almost the same as in Figure 4a; however, in this case some aggregate domains formed during the solution preparation are dispersed in the solution matrix. The aggregation is brought about by the creation of small  $\pi$ – $\pi$  stacked regions between the polymer segments and toluene that act as cross-links of the aggregate matrix (Figure 4b). The regions of the polymer–solvent  $\pi$ – $\pi$  complex in the aggregates are formed between statistically distributed successive parallel segments where the solvent molecules act as a bridge between them for efficient stacking. The orientation distribution of these associated segments are random, which being locked in a compact structure of the aggregate, can not reorganize into an aligned phase in the NMR to take a definite orientation with respect to the magnetic field; as a result the bound solvent gives rise to the three-line shape of the residual aromatic proton resonance which is upfield shifted due to the  $\pi$ – $\pi$  stacking. However, the solvent dynamics is much slower for these associated solvent molecules because of the  $\pi$ – $\pi$  stacking, causing relatively broad lines.

When the solution is brought to the subambient temperature, new aggregate domains develop in addition to the scenarios depicted in Figure 4, parts a and b, where the long axis of most of the segments is aligned parallel to each other (Figure 4c). Because of the magnetic susceptibility anisotropy of the rod-like segments of the polyfluorene backbone, their long axis tends to take a definite orientation relative to the magnetic field direction. This scenario is somewhat similar to the liquid crystal (LC) domain, excepting that the aligned segments have very little relative motion due to the connectivity of the segments in the aggregates. As a result of the local magnetic susceptibility and the lack of effective motional averaging, NMR signal from these aggregated polymer segments would be broad and featureless or with intensity below the noise level. However, such orientation of the aggregate matrix would establish a confined space where the trapped toluene molecules can exhibit anisotropic tumbling.<sup>38</sup> The latter would spin around the molecular axis ( $C_2$ ) taking a definite orientation relative to the field direction, giving rise to the motional averaged single sharp resonance (although still broader than that of the free toluene in the bulk solution) of the *para*-proton containing the said axis.

When we anneal the 0.5% solution at  $-20$   $^\circ\text{C}$ , the signal corresponding to the trapped solvent peak decays with time and ultimately disappears to the baseline as evidenced by the gradually reduced  $^1\text{H}$  NMR intensity with the annealing time (Figure 5a). This behavior indicates that the entrapment of the solvent



**Table 1.  $^1\text{H}$  Spin–Lattice Relaxation Times at 500 MHz for the Residual Protons of Toluene- $d_8$  in a 4.0% PF2/6 Solution Measured after Rapidly Cooling to  $-20\text{ }^\circ\text{C}$** 

proton ( $\delta$ ppm)	<i>meta</i> (7.12)	<i>para</i> (7.05)	<i>ortho</i> (6.99)	associated solvent (5.75)	$\text{CH}_3$ (2.09)
$T_1$ (s)	$3.02 \pm 0.72$	$2.86 \pm 0.65$	$3.00 \pm 0.71$	$0.30 \pm 0.071$	$2.42 \pm 0.61$

**Table 2. Structure and Dynamics of the Species in Different Phases of Toluene Solutions of PF2/6**

solvent	aggregate segments	solvent dynamics	solvent reorientation	solvent aromatic $^1\text{H}$ NMR shift
bulk	no aggregation	fast	isotropic	motional narrowed 3-line shape $\sim 7$ ppm
trapped	not aligned	slow	near isotropic	broad 3-line shape $\sim 6$ –5 ppm
trapped	LC type aligned phase	slow	anisotropic	single sharp line $\sim 6$ –5 ppm, temp sensitive

molecules is transient. The intensity profile of the signal (inset of Figure 5) shows that the approach to equilibrium follows a two-stage process. Furthermore, the linear decay suggests that the two processes are both of zeroth order, i.e., not dependent upon the concentration of the trapped solvent. The initial stage decays linearly up to  $\sim 110$  min followed by a steeper drop at a rate *ca.* 3.4 times that of the initial stage. The resonance line disappears after  $\sim 200$  min.

The question then arises as to why the associated solvent signal vanishes. This can simply be due to the fact that a large fraction of the entrapped solvent is expelled out of the aligned aggregates as the polymer segments become compact on aging at  $-20\text{ }^\circ\text{C}$ . Nevertheless, certain amount of the solvent molecules is always closely bound to the aggregate segments and their NMR intensity eventually disappears as their mobility decreases in a tight entrapment. By examining the intensity profile of the polymer backbone and the side-chains as a function of the annealing time shown in Figure 5b, we observe a loss of intensity of *ca.* 13% and 10% for backbone and side-chain protons, respectively, upon cooling to  $-20\text{ }^\circ\text{C}$  due to loss of motional narrowing upon aggregation. As the amount of the aggregated segments is quite appreciable, the entrapped solvent signal is apparent. The two-stage nature of the intensity loss of the signal suggests that two different mechanisms for the intensity loss are operative. The initial loss is likely due to expulsion of the excess solvent, which is a slow process. When most of the excess solvent is excluded, the parallel segments quickly densify

with the fluorenyl planes facing each other, and with the aromatic plane of toluene sandwiched between them, possibly in some slipped (offset) face-to-face geometry<sup>25,26</sup> where the methyl group of toluene stay outside the stack, avoiding any steric hindrance to the stacking. This forms a strong polymer–solvent  $\pi$ – $\pi$  complex where the reorientation of the aromatic plane of toluene about the  $C_2$  axis is hindered and ultimately becomes practically inaccessible in a tight entrapment. As a result of the lost mobility the entrapped solvent signal eventually vanishes. When the toluene approach closer to the fluorenyl plane, the residual aromatic protons experience a higher diamagnetic field from the ring current of the latter and consequently upfield shifted. At the same time the width of the trapped solvent line at half-maximum becomes larger as the molecules lose mobility when the segments densify with time. Both these facts are clearly evident in Figure 5c where the trapped solvent line has been shown as a function of the annealing time.

For a 5.3% solution of PF2/6 in toluene- $d_8$  mixed with 2% (v/v) pure toluene, the associated solvent appears as two overlapped lines contributed from the two solvents (Figure 6). Here the upfield shift of the associated solvent resonance is readily apparent as the segments densify. Another important feature of the resonance from this more concentrated solution is that it takes longer times to reduce the intensity and does not completely vanish even after 9 h of annealing. It is also noted that the two-stage nature of the drop of intensity is not prominent here (inset of Figure 6). This is because when the more concentrated solution is cooled the segments of the aggregates formed are much more crowded, making the diffusion of the excess solvent out of the aggregates difficult. The higher viscosity (due to chain entanglement) also prevents the parallel layers to assume the compact geometry quickly. In this case, the polymer–solvent complex can never attain a highly ordered compact structure, thereby still allowing the motion of some of the associated solvent molecules. As a result the associated solvent line can be observed even after 9 h of annealing.

We note here that the formation of the aggregates of aligned segments at subambient temperatures under the influence of the magnetic field and the transient entrapment of the solvent in them seem to be a characteristic of conjugated polymer solutions. We have observed that PF8 does not form aggregates in toluene solutions at ambient temperatures when the concentration is below 1%.<sup>22</sup> However when such a solution is brought to  $-20\text{ }^\circ\text{C}$  in the NMR probe, this polymer also forms aggregates of aligned segments in which some solvent is entrapped and behaves similarly to the PF2/6/toluene system with respect to the annealing phenomenon. For similar concentrations, however, the solvent entrapped in the PF8 aggregates diffuses out much quicker compared to the PF2/6/toluene system. Thus for a 0.57% solution it takes only about 40 min for the entrapped solvent signal to disappear (Supporting Information) compared to the 200 min required even for a slightly lower concentration in the PF2/6 case (Figure

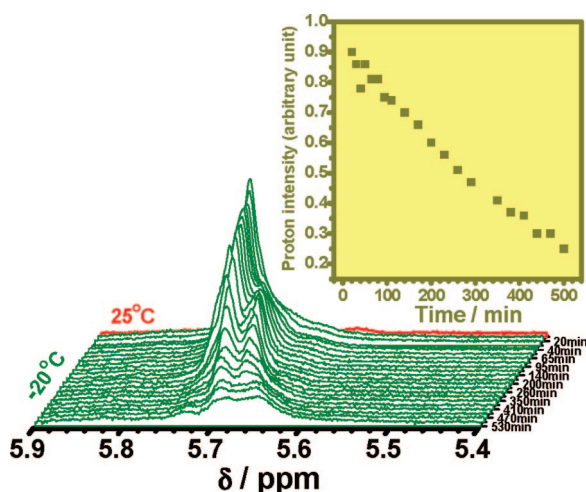


**Figure 6.** Selected portions of 500 MHz  $^1\text{H}$  NMR spectra of 5.3% PF2/6 solution in toluene- $d_8$  containing 2% (v/v) pure toluene taken at different aging times (shown against each spectra) at  $-20\text{ }^\circ\text{C}$ , cooled in one step from room temperature (top spectra in red, no associated solvent line). The associated solvent resonance contains overlapped lines due to the *para* proton of pure toluene and the residual *para* proton of deuterated toluene. Note that the last trace of the associated solvent line does not disappear completely even after 9 h of aging. Inset: Intensity of the line as a function of the annealing time.

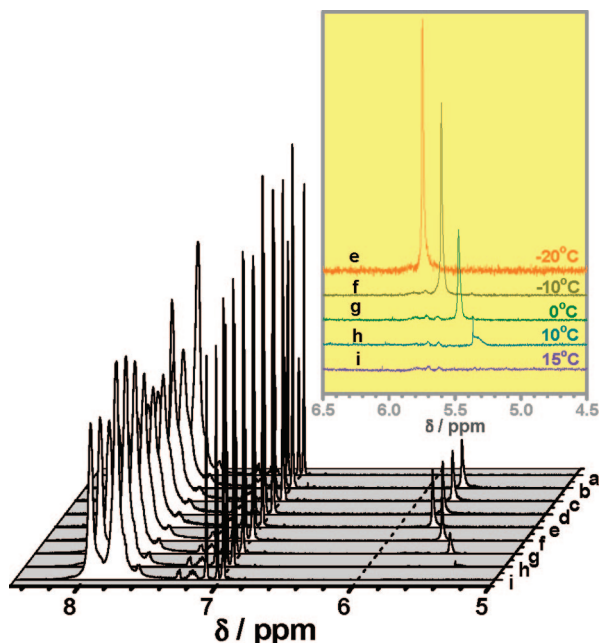


**Figure 7.** 500 MHz  $^1\text{H}$  NMR spectra of a 4.0% solution of PF2/6 in toluene- $d_8$ . The sample was rapidly cooled from 25  $^\circ\text{C}$  (a) to  $-20$   $^\circ\text{C}$  and was annealed there for 50 min during which spectra were taken at 15 (b), 25 (c), 40 (d), and 50 (e) min. The temperature was then increased stepwise to  $-10$ , 0,  $+10$ , and  $+15$   $^\circ\text{C}$  and spectra taken after 15 min at each step (f, g, h, and i, respectively). Inset: Expanded view of the associated solvent line region.

5a). This may indicate that the force for compaction of the segments at  $-20$   $^\circ\text{C}$  is much higher for the PF8 aggregates.

We have also carried out a temperature-programmed  $^1\text{H}$  NMR study for a 4.0% solution by cooling to  $-20$   $^\circ\text{C}$  and then annealing at this temperature for 50 min followed by a stepwise increase of the temperature (Figure 7). During the annealing the size of the entrapped solvent line reduces linearly as expected. However, during the heating process the intensity of the line rapidly diminishes and eventually disappears above 10  $^\circ\text{C}$  indicating that the aggregated state is dissipated at ambient temperatures. The entrapped solvent line shifts to higher fields as the temperature increases while the positions of all other resonance lines due to the polymer and the solvent remain mostly unperturbed. This is because the orientation of the molecular ( $C_2$ ) axis of associated toluene relative to the magnetic field largely determines the position of the line arising from the *para*-proton. Increase of the temperature changes the orientation of the molecular axis of toluene away from the magic angle ( $54.7^\circ$ , which we take as the reference point, as the orientation of the axis at this angle would produce the line exactly at the motional narrowed position). Consequently the line is shifted up-fields with increasing temperature. This is consistent with the 0.17 ppm less upfield shift of the line when the aggregates are formed at  $-30$   $^\circ\text{C}$  relative to that observed at  $-20$   $^\circ\text{C}$ . These results are in agreement with the notion that raising the temperature disrupts the segmental alignment of the aggregate domains, consequently their tendency to orient parallel to the field direction is weakened; i.e. raising the temperature moves the orientation away from the field direction.

Examining the intensity profile of the polymer backbone protons (Figure 8) we see a loss of about 24% of the room-temperature intensity due to the formation of the aggregates at  $-20$   $^\circ\text{C}$ . About 40% of this lost intensity is regained as we raise the temperature to  $-10$   $^\circ\text{C}$  (Figure 8b), due to the disruption of the less compact aggregates. Then the intensity remains fairly

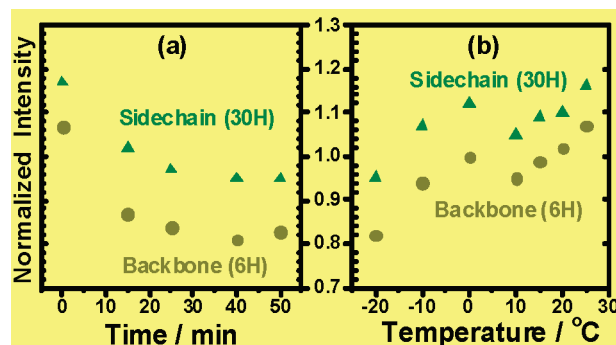


**Figure 8.** Normalized intensity of PF2/6 bands in  $^1\text{H}$  NMR spectra of a 4.0% solution with toluene- $d_8$  corresponding to the temperature program of Figure 7: (a) During aging for 50 min at  $-20$   $^\circ\text{C}$ , as a function of the time. The data at 0 min corresponds to 25  $^\circ\text{C}$ . (b) During the heating program, as a function of the temperature.

constant up to about 15  $^\circ\text{C}$ , after which the intensity increases linearly with the rise of the temperature and the room-temperature intensity is completely recovered at 25  $^\circ\text{C}$ . This means that the well ordered compact polymer-solvent  $\pi$ - $\pi$  complexes are stable up to 15  $^\circ\text{C}$  and they are disrupted only above this temperature. During this period of the temperature program (between  $-10$  and  $+15$   $^\circ\text{C}$ ), the aggregates release the entrapped solvent and the segments densify with consequent intensity loss, similarly to the annealing experiments. The complete recovery of the room temperature intensity of the polymer proton resonances when reheated back to 25  $^\circ\text{C}$  displays the thermoreversible nature of the aggregates.

## Conclusion

We introduce an efficient  $^1\text{H}$  NMR method for studying the interaction and dynamics of the aggregate domains of conjugate polymer solutions. From the information gathered on the PF2/6/toluene system, we conclude that the segmental aggregation is stabilized by the formation of polymer-solvent complex through  $\pi$ - $\pi$  interaction between the polymer segments and the solvent firmly associated with them. The plane of the aromatic ring of toluene get sandwiched between two successive layers of polymer segments facilitating the stacking of the polymer segments in the complex that are otherwise unsuitable for the  $\pi$ - $\pi$  stacking due to steric hindrance from the side-chains attached to each repeating unit. This causes a separate resonance for the residual aromatic protons of the associated toluene in  $^1\text{H}$  NMR, upfield shifted from the motional narrowed aromatic proton lines of the bulk solvent, facilitating the characterization of the aggregates. The magnetic field of the NMR forces the polymer segments in the aggregate domains to take a definite orientation of their long axis relative to the direction of the field, in a manner similar to a liquid crystal domain. The associated toluene molecules in this highly anisotropic magnetic environment also get a definite orientation of their molecular  $C_2$  axis relative to the field direction. The bound solvent molecules, however, are under exchange equilibrium with the free ones, which is rapid on the dipolar coupling time scale, causing decoupling and the appearance of only one sharp resonance line for the *para* proton of the associated toluene, the position of which is sensitive to the temperature as a change in the temperature changes the orientation of the molecule. Initially a large excess of the solvent are entrapped within the aggregates when the temperature is lowered to below ambient. The approach to equilibrium follows a two-step mechanism: diffusion of the



excess solvent in a slow step followed by rapid compaction of the polymer–solvent  $\pi$ – $\pi$  complex. The compact aggregates are stable up to 15 °C above which they dissipate and the room-temperature intensity of the polymer resonances are recovered, displaying the thermoreversible nature of the aggregation.

**Acknowledgment.** This work was supported by the National Science Council (NSC) of Taiwan under grant numbers NSC 95-2752-E-007-006-PAE and NSC 94-2218-E-007-049. M.H.R.

acknowledges the NSC for financial support in the form of a postdoctoral fellowship. He also acknowledges the University of Rajshahi, Bangladesh, for granting him study leave during the study.

**Supporting Information Available:** Figure showing the  $^1\text{H}$  NMR spectra of a toluene- $d_8$  solution of 0.57% (w/v) PF8 at  $-20$  °C with varying annealing times. This material is available free of charge via the Internet at <http://pubs.acs.org>.

LA802526D